

Ghost imaging protocol with intense correlated fields for efficient encryption

E. Puddu¹, I. P. Degiovanni^{2,†}, A. Andreoni¹, M. Bondani³, and S. Castelletto²¹Dipartimento di Fisica e Matematica,
Università degli Studi dell'Insubria and
Consiglio Nazionale delle Ricerche,
Istituto Nazionale per la Fisica della Materia (C.N.R.-I.N.F.M.),
Via Valleggio, 11 - 22100 Como, Italy²Istituto Nazionale di Ricerca Metrologica,
Strada delle Cacce 91 - 10135 Torino (Italy)³National Laboratory for Ultrafast and Ultraintense Optical Science - C.N.R.-I.N.F.M.,
Via Valleggio, 11 - 22100 Como, Italy
(Dated: November 27, 2018)

We present a proof of principle of a straightforward application of distributed imaging to the efficient encryption of images. The basic idea is to exploit, in a ghost-imaging experiment, the correlations of the fields produced by a chaotically seeded parametric downconversion to deduce a Code for reconstructing the image of the object. As this Code results to be much smaller than the entire image size, it can be more efficiently encrypted by any secure quantum key.

PACS numbers: 42.50.-p, 42.65.Lm, 03.67.Dd, 03.67.Hk

Quantum key distribution (QKD) is a direct application of fundamental quantum mechanics, involving two parties, Alice and Bob, exchanging some classical information. By QKD Alice and Bob exchange secret random keys to implement a secure encryption-decryption algorithm (one-time-pad) without meeting, and the security of the distributed keys is based on the laws of quantum physics [1]. However at variance with classical communication that can be performed at a rate of G byte/s, though in an insecure way, practical QKD protocols, in their up-to-date best realizations, allow secure quantum key rates below 10 K bit/s, possibly improved to 100 K bit/s in the next ten years [2]. Therefore, as the length of the key must necessarily equal the length of the message to guarantee absolute security, for a real world application quantum keys can be used only for encrypting the most sensitive parts of the messages. In protocols for secure image transmission [3, 4, 5], the problem cannot be easily bypassed because any image must be encrypted as a whole.

Here we propose a proof of principle experiment to solve the problem that the usual size of an image requires a long secure quantum key by using the properties of a ghost imaging protocol with intense correlated fields. Ghost imaging capability was initially attributed only to entangled photon pairs [6], but in more recent works it has been ascertained also for classically correlated fields, both in the single photon regime [7, 8, 9] and in the continuous variable regime [10, 11]. The main result of all these schemes is the non-local imaging of the object both in near- and far-field [12]. In all the mentioned schemes, the technique adopted for the retrieval of the image consists of the measurement and the evaluation of

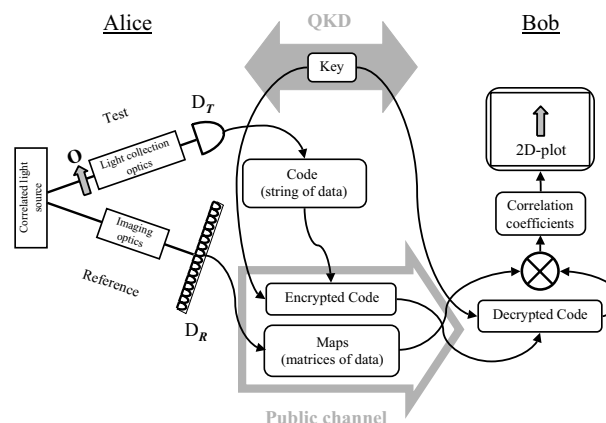


FIG. 1: Scheme of an efficient encryption of the image of an object by distributed imaging.

the fourth-order correlation between the correlated fields.

In our scheme, the measurements performed at Alice's laboratory are the following ones (see Fig. 1): the beam containing the object (Test-arm beam) is measured with a bucket detector, D_T , which does not provide any spatial information, while the other beam (Reference-arm beam) is either scanned with a pointlike detector or measured by a position sensitive detector, such as a CCD camera, D_R . Neither of the two sets of data collected separately carries information that is suitable to recognize the object, but they represent a pair of complementary sets from which Bob will univocally determine the object image. In our picture one of the sets serves as the Code to convert the information carried by the other set into the image of the real object. As the Code, we adopt the data set recorded on the Test arm, which is a string of numbers,

† Electronic address: emiliano.puddu@uninsubria.it

‡ Electronic address: degio@ien.it

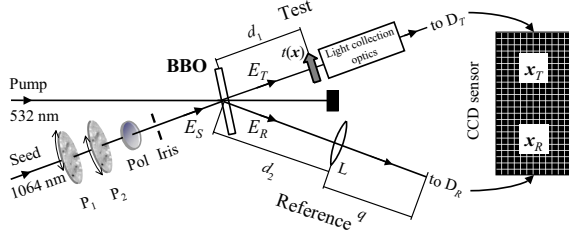


FIG. 2: Experimental setup: $P_{1;2}$, independently rotating ground glass plates; Pol, polarizer; $t(x)$, object transmission function; L, lens. The CCD sensor is used to detect both Test and Reference beams.

whereas the set of M maps recorded on the Reference arm is a collection of two-dimensional matrices of data. In our protocol the Code undergoes QKD, while the two-dimensional matrices are sent on a non-jammable public channel. As shown in Fig. 1, Alice and Bob exchange a quantum cryptographic Key by using a QKD protocol (e.g. BB84 and B92). Alice owns the object of which she wants to securely transmit the image to Bob. She records N chaotic Maps and the corresponding N values of optical power, that are the Code. Via a public non-jammable channel, Alice sends Bob the sequence of the M maps and the Code encrypted by the Key. Bob decrypts the Code, performs the calculation of the fourth-order correlation coefficients between the M maps and the Code and obtain 2D-plots that display the recovered image.

We realized the ghost-imaging experiment by using two intense beams generated by a seeded difference-frequency⁽²⁾ process. In Fig. 2 we show our experimental setup. We injected a coherent collimated pump beam (532 nm) and a seed beam (1064 nm) into a crystal of $\text{-BaB}_2\text{O}_4$ (BBO, cut angle 22.8 deg; (10 mm 10 mm 2 mm), Fujian Castech Crystals, China). Both pump and seed beams are provided by an amplified Q-switched Nd:YAG laser (GCR-4, 10 Hz repetition rate, 7 ns pulse duration of the fundamental pulse, Spectra-Physics, USA). In order to obtain the desired chaotic statistics, the seed field was randomized by passing it through two independently rotating ground glass plates, P_1 and P_2 [13]. The nonlinear process generates a field at frequency degeneracy (Reference), which has a precise phase relation to the amplified seed field (Test). In both Reference and Test arms we measured the photon number statistics and found perfect agreement with the expected chaotic statistics [14, 15].

As the detector, we used a single CCD camera (CA-D 1-

256T, (16 16) m^2 pixel area, 12 bit resolution, Dalsa, Canada) whose sensor, also depicted in Fig. 2, for one half recorded the single-shot intensity Maps in the Reference arm, $I_R(x_R)$, and for the other half realized the bucket detector of the Test arm. In the following, I_T designates the sum of the contents of the pixels. The Test arm includes free propagation over distance $d_1 = 60$ cm from the BBO to the object, object transmission function $t(x)$, and light collection optics in front of the bucket detector. The Reference arm contains free propagation from BBO to L (distance $d_2 = 60$ cm, focal length $f = 400$ mm) and from L to the CCD camera (distance q). Distances d_1 , d_2 and q must satisfy the thin lens equation:

$$\frac{1}{d_1 + d_2} + \frac{1}{q} = \frac{1}{f} \quad (1)$$

to give an imaging system with magnification factor $M = q/(d_1 + d_2)$. In our case $M = 0.5$. The technique adopted to recover the image is the computation of the shot-to-shot correlation coefficients of the total I_T measured by the bucket detector and the intensity values detected in the Reference arm at position x_R , that is [10]:

$$G(I_R(x_R); I_T) = \overline{h_I(x_R) I_T} - \overline{h_I(x_R)} \overline{h_I} \quad (2)$$

where $\overline{\cdot}$ denotes the average over a number of subsequent laser shots. The technique works as, being the seed field E_S made chaotic, also the generated field E_R is chaotic [16] and all complex amplitudes are described by gaussian complex random variables [17, 18]: this implies the strong intensity correlations between E_T and E_R that we exploited for our purposes. For both arms we write the propagation from the nonlinear crystal to the detectors as

$$E_i(x_i) = \int_Z dx_i^0 h_i(x_i; x_i^0) E_i^0(x_i^0); \quad i = T; R \quad (3)$$

where $h_i(x_i; x_i^0)$ are the proper transfer functions. By taking into account that $G(I_R(x_R); I_T) = \int dx_T G(x_R; x_T)$ we calculate

$$\begin{aligned} G(x_R; x_T) = & \int_Z \int_Z \int_Z \int_Z dx_T^0 dx_T^{00} dx_R^0 dx_R^{00} h_T(x_T; x_T^0) h_R(x_R; x_R^0) \\ & \overline{h_T(x_T; x_T^0) h_R(x_R; x_R^0) h_T(x_T; x_T^{00}) h_R(x_R; x_R^{00})} \\ & \overline{h_T(x_T^0) E_T(x_T^0) E_R(x_R^0) E_R(x_R^{00})} \\ & \overline{h_T(x_T^{00}) E_T(x_T^{00})} \overline{h_R(x_R^0) E_R(x_R^0)} \overline{h_R(x_R^{00}) E_R(x_R^{00})} \end{aligned} \quad (4)$$

The observation that in the linear-gain regime and under the hypothesis of thin crystal, the complex amplitudes of the macroscopic fields can be written as $E_T(x) \propto E_S(x)$ and $E_R(x) \propto E_S(x)$, along with the properties of gaussian statistics, yields

$$\begin{aligned} G(x_R; x_T) = & \int_Z dx_T^0 dx_R^0 h_T(x_T; x_T^0) h_R(x_R; x_R^0) \\ & G^{(1;1)}(x_R^0; x_T^0) \end{aligned} \quad (5)$$

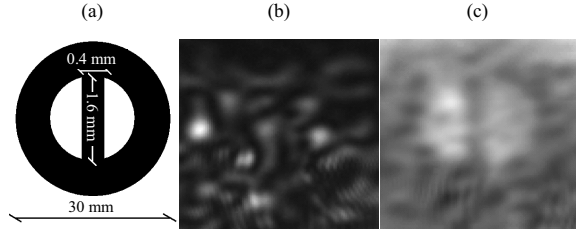


FIG. 3: (a) Drawing of the object transmission function $t(x)$ located on the Test-arm of the experimental setup. (b) Typical sample of chaotic single-shot Map $I_R(x_R)$ recorded on the Reference-arm. (c) Image of $t(x)$ recovered by evaluating $G(I_R(x_R); I_T)$ over 2500 laser shots. The size of the maps in (b) and (c) is $(126 \times 130 \text{ pixels}^2 = 2.016 \times 2.080 \text{ mm}^2)$.

where $G^{(1;1)}(x_R^0; x_T^0)$ is the first order correlation between $E_T(x_T^0)$ and $E_R(x_R^0)$. By using the input-output relations of above and considering the temporal and spatial incoherence of the seed field, we can write:

$$\begin{aligned} G^{(1;1)}(x_R^0; x_T^0) &= \langle hE_R(x_R^0)E_T(x_T^0) \rangle_i \\ &= \frac{\langle hE_S(x_R^0)E_S(x_T^0) \rangle_i}{I_S(x_R^0)I_S(x_T^0)} (x_T^0, x_R^0) : (6) \end{aligned}$$

Substituting Eq. (6) into Eq. (5) gives:

$$G(x_R; x_T) / \int dx_R^0 I_S(x_R^0) h_T(x_T; x_R^0) h_R(x_R; x_R^0) : (7)$$

As in our setup $I_S(x_R^0)$ can be taken as independent of x_R^0 and the transfer functions are simple, it is trivial to perform the integration and show that:

$$G(I_R(x_R); I_T) / \int (M x_R) \int^2 (8)$$

In Fig. 3 we show the experimental results obtained by calculating the averages in Eq. (2) on 2500 recorded

chaotic images: panel (a) shows a drawing of the transparency $t(x)$, (b) shows a typical sample of chaotic single-shot Map $I_R(x_R)$, and (c) shows the image recovered by plotting $G(I_R(x_R); I_T)$.

Let us analyze the experimental results from the point of view of efficient encryption and image transmission. Storing the information of the reconstructed image requires 104 K bytes, whereas storing the Code requires 22 K bytes. This means that by using our protocol, in which only the Code must be securely encrypted, we achieve a reduction of about 80% of the required quantum Key length. We performed a test in which we used a standard PC data compression program, obtaining that the compressed file of the image is reduced to 44 K bytes. This size should be compared with the 22 K bytes size of our Code file which, once compressed, reduced to 9 K bytes.

Moreover, we want to underline that the number of the elements of the Code necessary to reconstruct an image is independent of the dimension of the image itself: in fact the number of elements corresponds to the number of chaotic images on which Bob computes the correlation coefficients to obtain the reconstructed intensity map. As the pixels of the correlation maps are reconstructed independently of each other, the size of the statistical ensemble on which we must calculate the averages in Eq. (2) are simply determined by the noise in the measurement. This means that, in principle, the advantage of using this scheme can be strongly enhanced with respect to the 80% obtained in the experiment of above in the case of bigger maps (and pictures).

In conclusion, as QKD for secure image transfer is a difficult task, in order to reduce the key consumption we proposed a scheme for an efficient encryption of images that exploits distributed imaging techniques. We performed an experiment of ghost imaging based on the correlations of the fields produced by a chaotically seeded parametric downconversion to produce a set of chaotic images and a Code, both necessary for reconstructing the image of the object. In a proof of principle we observed that the information storage of this Code resulted to be much smaller than that of the entire image. Thus the Code can be more efficiently encrypted by any secure cryptographic Key and sent to the legitimate receiver, who will be able to reconstruct the image by using the decrypted Code together with the publicly announced chaotic images.

- [1] N. Gisin, G. Ribordy, W. Tittel and H. Zbinden, Rev. Mod. Phys. 74, 145 (2002).
 [2] "A Quantum Information Science and Technology roadmap. Part 2: Quantum cryptography" version 1.0, ARDA (2004), <http://qist.lanl.gov>.
 [3] A. Zeilinger, Rev. Mod. Phys. 71, 288 (1996).
 [4] T. Jennewein, C. Simon, G. Weihs, H. Weinfurter, and

- A. Zeilinger, Phys. Rev. Lett. 84, 4729 (2000).
 [5] R. J. Hughes, J. E. Nordholt, D. Derkacs and C. G. Peterson, New J. Phys. 4, 43, (2002).
 [6] T. B. Pittman, Y. H. Shih, D. V. Strekalov, A. V. Sergienko, Phys. Rev. A, 52, R 3429 (1995).
 [7] R. S. Bennink, S. J. Bentley, and R. W. Boyd, Phys. Rev. Lett. 89, 113601 (2002).

- [8] Yan-Hua Zhai, Xi-Hao Chen, Da Zhang, and Ling-An Wu, *Phys. Rev. A* 72, 043805 (2005).
- [9] J. Cheng and S. Han, *Phys. Rev. Lett.* 92, 093903 (2004).
- [10] A. Gatti, E. Brambilla, and L. A. Lugiato, *Phys. Rev. Lett.* 90, 133603 (2003).
- [11] F. Ferri, D. Magatti, A. Gatti, M. Bache, E. Brambilla, and L. A. Lugiato, *Phys. Rev. Lett.* 94, 183602 (2005).
- [12] M. D'Angelis and Y. H. Shih, *Laser Phys. Lett.* 2, 567 (2005) and references therein.
- [13] F. T. Arecchi, *Phys. Rev. Lett.* 15, 912 (1965).
- [14] E. Puddu, A. Levi, M. Bondani, and A. Andreoni, *Opt. Letters* 10 1294 (2005).
- [15] M. Bondani, E. Puddu, and A. Andreoni, *J. Mod. Opt.* 53, 761 (2006).
- [16] B. R. Mollow and R. J. Glauber, *Phys. Rev.* 160, 1076 (1967).
- [17] L. Mandel and E. Wolf, *Optical Coherence and Quantum Optics* (Cambridge University Press, New York, 1995).
- [18] J. W. Goodman, *Statistical Optics* (Wiley-Interscience, New York, 1985).